Fermilab Library
0 1160 0025526 9

IMPERIAL
TP/92-93/14

Imperial/TP/92-93/14

Optimization in the Extended Variational Approach: The SU(2)-SO(3) Phase Structure on the Lattice

J. O. Akeyo and H. F. Jones
Physics Department, Imperial College, London SW7 2BZ, UK.

Abstract

We use the linear delta expansion with a trial action based on single links to explore the phase structure of the mixed SU(2)-SO(3) lattice gauge theory. The method can be regarded as a systematic expansion going beyond mean field theory or the variational method, to which it is closely related in first order. At $O(\delta^2)$ the line of first-order phase transitions is shown to terminate, and at $O(\delta^3)$ the boundaries between the different phases are well reproduced.

1. Introduction

The linear delta expansion (LDE) is a promising new analytic approach to field theory [1] which has been successfully applied to a variety of problems of a non-perturbative nature. In its basic construction, the LDE includes an arbitrary parameter λ in the action. Physical quantities are evaluated by optimizing λ. The LDE is a systematic expansion which enables one to go beyond the conventional variational method.

The method consists in constructing an action S_δ interpolating linearly between the action S of the theory and the action S_0 of a soluble theory chosen to reflect as much of the physics of S as possible. We have

$$\begin{aligned} S_\delta &= \delta S + \lambda(1-\delta)S_0 \\ &= \lambda S_0 + \delta(S - \lambda S_0). \end{aligned}$$

It is clear that $S_{\delta=0} = \lambda S_0$, while $S_{\delta=1} = S$, independent of λ . The vacuum generating functional and the appropriate expectation values are then evaluated as truncated expansions in δ, which is then set equal to unity in the end.

While the infinite sum is independent of λ, the truncated expansion has a nontrivial dependence on λ. We must therefore choose the optimum value of λ. The principle of minimal sensitivity (PMS)[2] has been adopted as the optimization criterion which minimizes the dependence on λ of the result being calculated. If $R_K(\lambda)$ is the result truncated at order K, the criterion reads

$$\frac{\partial R_K}{\partial \lambda} = 0.$$

Besides generating the non-perturbative character of the LDE, this optimization criterion produces a convergent sequence of approximants out of what would otherwise be an asymptotic or divergent series (see refs. [3] and [4] for a proof of the convergence of the LDE in low dimensions).

With various choices of the trial action S_0, the LDE has been applied to the calculation of the plaquette energy, E_P, of lattice gauge theories [5-7], with results in good agreement with Monte Carlo (MC) measurements both in the strong-coupling and weak-coupling regimes.

Recently [8], we applied the LDE to the calculation of the plaquette energy of the SU(2) gauge theory on the lattice with a trial action based on single links, namely

$$S_0 = J \sum_\ell \mathrm{tr}\, U_\ell$$

with $J \equiv \lambda$. By applying the optimization criterion $\partial E_P/\partial J = 0$ to the plaquette energy E_P, calculated up to $O(\delta^3)$, we obtained results in very good agreement with

MC results. This success has encouraged us to apply the method to more complicated quantities and features.

In this paper, we have applied the LDE to the study of the phase structure of the mixed SU(2)–SO(3) pure gauge theory on the lattice. Monte Carlo calculations [9–11] have revealed a rich phase structure for this system, with a line of first-order phase transitions ending at a critical point just before reaching the SU(2) axis.

While the SU(2) system in the fundamental representation does not undergo a phase transition, the SO(3) system has a first order phase transition as it passes from the strong-coupling into the weak-coupling region. The non-deconfining first order phase transitions in the SO(3) and the mixed SU(2)–SO(3) pure gauge systems have been ascribed to a condensation of Z_2 monopoles, as confirmed by MC measurements [11–15]. The point $\beta \simeq 2.2$ where the specific heat of the fundamental SU(2) system develops a sharp peak has been interpreted as a remnant of the nearby critical end-point [9] in the SU(2)–SO(3) phase diagram. This conjecture has been confirmed [13] by an explicit MC measurement of the specific heat of the mixed system.

Analytically, the system has been studied by a variety of techniques. Zeroth-order mean field [16,17] and first-order variational [18] methods reveal the expected phase structure, but fail to produce the critical end-point observed in MC experiments; the line of first-order phase transitions crosses the fundamental SU(2) axis. Mean field with one-loop Gaussian corrections and gauge fixing ($U_\ell = 1$ in a particular direction) [19,20] as well as the mean-plaquette [21] and the strong-coupling expansion methods [22] produce the desired end-point with varying degrees of accuracy. Renormalization-group techniques of the Migdal-Kadanoff type have also been applied [23] to produce a phase structure for the mixed SU(2)–SO(3) system in excellent agreement with MC measurements.

In a study devoted to the investigation of the mechanism causing first-order phase transitions in the mixed SU(N) lattice gauge systems, Bachas and Dashen [24] observed that in four dimensions, "the existence of non-trivial, non-degenerate minima of the one-plaquette action gives rise to a first-order phase transition and the critical end-point of the line of these first-order phase transitions occurs where the non-trivial local minima become unstable". We will return to this point in section 3.

The details of the model and the calculational framework are explained in section 2. Section 3 contains the results of our calculations, which are displayed graphically in Figs. 1 -3. Our conclusions follow in section 4. In the course of this investigation we developed a new method of calculating the required expectation values with respect to the single-link trial action S_0. This method, which makes the evaluation of higher-order correlations much simpler, is presented in an appendix.

2. The Model

We consider a mixed fundamental-adjoint SU(2), i.e., SU(2)–SO(3) pure gauge theory on a four-dimensional hypercubic lattice with action

$$S = \beta \sum_P \mathrm{tr}\, U_P + \frac{1}{3}\beta_A \sum_P \mathrm{tr}_A U_P \tag{1}$$

where tr (tr_A) denotes the trace in the fundamental (adjoint) representations of the SU(2) gauge group. β (β_A) is the coupling constant for the SU(2) (SO(3)) system and U_P is the usual product of group link elements around elementary plaquettes of the lattice.

This mixed system has three limits:

(i) $\beta_A = 0$ – the usual Wilson SU(2) theory

(ii) $\beta = 0$ – the action only depends on the adjoint representation corresponding to the standard Wilson SO(3) gauge theory

(iii) $\beta_A = \infty$ – all plaquette variables in the SO(3) gauge group are driven to the identity. Each plaquette variable in the SU(2) system must then lie in the centre of the gauge group, i.e. $U_P \in \pm I$. Hence, up to a gauge transformation, all link variables belong to the centre of the group[9]. In this limit we thus obtain a Z_2 lattice gauge theory. Both SO(3) and Z_2 lattice gauge systems undergo first-order phase transitions, and therefore we expect lines of first-order phase transitions to enter the mixed SU(2)–SO(3) system from the $\beta = 0$ and the $\beta_A = \infty$ axes.

We use the following identity between the adjoint and fundamental representations:

$$\mathrm{tr}_A U = (\mathrm{tr}\, U)^2 - 1 \tag{2}$$

All our calculations are then in terms of traces in the fundamental representation.

In the continuum limit the SU(2) and SO(3) lattice actions are the same. The main difference between the two systems is that SU(2) distinguishes between $+U, -U$, while SO(3) does not. To take account of this fact we introduce the Z_2 (centre) degrees of freedom explicitly on each link ℓ of the lattice and write

$$U_\ell \to U_\ell \sigma_\ell, \quad U_P \to U_P \sigma_P. \tag{3}$$

where $\sigma_\ell = \pm 1 \in Z_2$, $\sigma_P = \prod_{\ell \in P} \sigma_\ell$. Therefore the model we adopt to study the phase structure of the mixed fundamental-adjoint SU(2) action is

$$S = \beta \sum_P \mathrm{tr}\,(U_P \sigma_P) + \frac{1}{3}\beta_A \sum_P [(\mathrm{tr}\, U_P)^2 - 1]. \tag{4}$$

For our trial action we choose a mixed single-link SU(2) and Z_2 action given by

$$S_0 = J\sum_\ell \mathrm{tr}\, U_\ell + m\sum_\ell \sigma_\ell. \tag{5}$$

where J and m are arbitrary parameters, taken to be the same on all the links of the lattice. As illustrated in the appendix, we treat the SU(2) and the Z_2 elements separately in evaluating the appropriate expectation values with respect to the trial action S_0.

The linear interpolating action is then given by

$$S_\delta = S_0 + \delta(S - S_0). \tag{6}$$

The trial partition function is given by

$$\begin{aligned} Z_0 &= \int \prod_\ell dU_\ell \prod_\ell (\frac{1}{2}\sum_{\sigma_\ell=\pm 1}) e^{S_0} \\ &= [f(J)]^{N_\ell}[g(m)]^{N_\ell}. \end{aligned} \tag{7}$$

where $f(J) = I_1(2J)/J$ and $g(m) = \cosh m$. N_ℓ is the total number of links and $I_r(x)$ is the modified Bessel function of order r. The connected vacuum generating functional is then evaluated as an expansion in the parameter δ, i.e.,

$$\begin{aligned} Z = e^{-W} &= \int \prod_\ell dU_\ell \prod_\ell (\frac{1}{2}\sum_{\sigma_\ell=\pm 1})\, e^{S_0} e^{\delta(S-S_0)} \\ &= Z_0 < e^{\delta(S-S_0)} >_0 . \end{aligned} \tag{8}$$

W is the free energy of the system, and the expectation value of a variable X w.r.t. S_0 is defined as

$$< X >_0 = \frac{1}{Z_0}\int \prod_\ell dU_\ell \prod_\ell (\frac{1}{2}\sum_{\sigma_\ell=\pm 1}) e^{S_0} X. \tag{9}$$

Expanding the exponential in eq. (8) gives the free energy

$$W = W_0 - \sum_{n=1}^{\infty} \frac{\delta^n}{n!} < (S - S_0)^n >_C . \tag{10}$$

where the subscript C denotes the connected expectation value. This expansion will be truncated at some finite order K, and δ then set equal to 1.

To monitor the behaviour of the system, we have calculated the free energy per link, F, and the order parameters E_F and E_A defined by

$$F = \frac{1}{N_\ell}W = \frac{1}{N_\ell}W_0 - \sum_{n=1}^{\infty}\frac{\delta^n}{n!} < (S - S_0)^n >_C, \tag{11}$$

$$\begin{aligned} E_F &=< \frac{1}{2}\mathrm{tr}\,(U_P\sigma_P) >= -\frac{1}{N_\ell(d-1)}\frac{\partial F}{\partial \beta}, \\ E_A &=< \frac{1}{3}\mathrm{tr}_A U_P >= -\frac{2}{N_\ell(d-1)}\frac{\partial F}{\partial \beta_A}. \end{aligned} \tag{12}$$

We note that $W_0 = -\ln Z_0$ and d is the number of space-time dimensions, equal to four in our calculations. We have worked in the temporal gauge.

In the LDE, the free energy and the order parameters of a lattice gauge system always have a local minimum (maximum) around $J = 0$ ($m = 0$) associated with the strong-coupling limit of the theory. This trivial minimum remains the only local minimum within the strong-coupling region. But as soon as we cross from the strong-coupling into the weak-coupling region a nontrivial local minimum of the free energy (order parameter) suddenly appears at $J \neq 0$ ($m \neq 0$). In our optimization scheme, this nontrivial minimum (maximum) is normally the PMS stationary point at which we obtain the value of the physical quantity in the weak-coupling region. The fact that a nontrivial local minimum occurs suddenly as we cross from the strong-coupling into the weak-coupling region can be used to estimate the location of a phase transition point in lattice gauge theory.

Thus for the mixed SU(2)-SO(3) lattice gauge theory, we have determined phase transition points by applying the PMS optimization criterion:

$$\frac{\partial R_K}{\partial J} = 0; \quad \frac{\partial R_K}{\partial m} = 0 \tag{13}$$

for the three separate cases $R = F$, E_F, E_A. At a transition point the free energy $F \leq 0$.

To determine the phase transition points in the two-coupling space of the mixed system, we fix β, say, and vary β_A until a nontrivial local minimum just appears or disappears depending on which side of the coupling, strong or weak, we approach it from. Such a point (β, β_A), where the PMS point just appears or disappears is a phase transition point.

All the phase transition points we have determined in this way are first order – the physical properties of the system change discontinuously at the transition points. We thus find lines of first-order phase transitions separating the strong-coupling and the weak-coupling regions of the mixed fundamental-adjoint SU(2) pure gauge theory.

3. Phase Structure of The Mixed Action

Using Eqs. (4), (5), (7), (11) and (12), we have calculated expressions for the free energy and order parameters of the system. To study the phase structure of our model in the various coupling limits, we consider the following expressions for the $O(\delta)$ free energy and the $O(\delta)$ order parameters (corresponding to $O(\delta^2)$ free energy) calculated for the moment without gauge fixing:

(i)

$$F = F_0 + 2JV_2 + mt - \frac{3}{2}(\beta C_1 t^4 + \beta_A V_3^4) \tag{14}$$

where $F_0 = -(1/N_\ell)\ln Z_0 = -\ln(I_1(2J)/J) - \ln(\cosh m)$

(ii)

$$E_F = \frac{1}{2}C_1 t^4 - \frac{1}{2}JC_1' t^4 - 2mt^3 C_1(1-t^2) + \frac{1}{2}\beta(D_{21} - C_1^2 t^8 + 20t^6(D_{22} - C_1^2 t^2)) + \frac{1}{6}\beta_A t^4(D_{31} - C_1 D_{21} + 20(D_{32} - C_1 D_{21})) \tag{15}$$

(iii)

$$E_A = V_3^4 - \frac{1}{3}JD_{21}' + \frac{1}{9}\beta_A(D_{41} - D_{21}^2 + 20(D_{43} - D_{21}^2)) + \frac{1}{3}\beta t^4(D_{31} - C_1 D_{21} + 20(D_{32} - C_1 D_{21})) \tag{16}$$

where C_1, D_{ij} denote plaquette diagram correlation functions with respect to the single-link SU(2) trial action and the primes represent first-order differentiations w.r.t. J. We give in the appendix the definitions and complete expressions for these diagrams. In general they are functions of ratios of the modified Bessel functions of the form, $V_r = I_r(2J)/I_1(2J)$. We have denoted $t = \tanh m$.

In the limit $\beta_A = 0$ ($\beta = 0$), Eqs. (14-16) reduce to the respective expressions describing the SU(2) (SO(3)) pure lattice gauge theories to $O(\delta)$. The limit $\beta_A = \infty$ is less trivial. In this limit, $J = \infty$, and the modified Bessel function ratios $V_r = 1$, with their derivatives w.r.t. J equal to zero. Using this property in Eqs. (15) and (16), we obtain

$$E_A = 1$$

and

$$E_F = t^4 + 2\beta(1 - t^8 + 20t^6(1-t^2)) - 4mt^3(1-t^2) = <\sigma_P>. \tag{17}$$

Hence in the limit $\beta_A = \infty$, the mixed system is in the weak-coupling region of the SO(3) gauge theory and the order parameter E_F reduces directly to the expression

for the plaquette energy for the Z_2 lattice gauge theory in the LDE (or variational cumulant expansion) with action

$$S_Z = \beta \sum_P \sigma_P. \tag{18}$$

and trial action

$$S_{0m} = m \sum_\ell \sigma_\ell$$

This confirms explicitly that in the limit $\beta_A = \infty$, the mixed SU(2)–SO(3) pure lattice gauge system reduces to a Z_2 pure lattice gauge system. We therefore have three distinct phase regions, as observed earlier. It is remarkable to note that with the choice of the single-link SU(2) trial action in the LDE, the Z_2 gauge system emerges very simply from the properties of the modified Bessel function ratios in the limit $\beta_A = \infty$ ($J = \infty$).

In the temporal (axial) gauge, we set all link elements $U_\ell \to U_\ell \sigma_\ell = 1$ in the time direction, so that only elements on the spatial links are active. This differs slightly from the gauge fixing procedure adopted in the mean field methods [19] where the Z_2 elements have been kept active on all links, both spatial and temporal.

To $O(\delta)$ our expression for the free energy is exactly the same as that obtained in the variational method [18], and without gauge fixing (eq. (14)) gives precisely the same results for the phase diagram, since at this order the LDE optimization procedure coincides with the variational principle used as a criterion in determining the phase transition points in the variational method. However, in the temporal gauge, our $O(\delta)$ free energy gives a much better picture of the phase structure of the system compared to the variational and mean field results [18-20] at this order, even though a line of first-order phase transitions crosses the fundamental SU(2) axis ($2\beta \simeq 2.34$)— at a point where there is normally some activity in the SU(2) gauge system. This result does not agree with the Monte Carlo picture, as explained in the introduction. At this order in the LDE the order parameters are trivial and cannot be used to monitor the behaviour of the system using the optimization criterion of eq. (13).

Taking the calculation to $O(\delta^2)$ in the free energy and $O(\delta)$ in the order parameters, and applying eq. (13), we obtain much improved results in general agreement with the MC picture. The optimization criterion produces an end-point observed in the MC measurements at this order in the LDE. The $O(\delta^2)$ free energy and the corresponding order parameters now locate the phase transition point on the SO(3) axis at $\beta_A \simeq 2.533$, very close to the MC point $\beta_A \simeq 2.5$. We locate an end-point within the same region as the MC observation; our end-point occurs at $(2\beta, \beta_A) \simeq (1.5, 0.73)$ and

$(2\beta, \beta_A) \simeq (1.64, 0.9)$ determined with free energy and order parameters respectively. The MC end-point [†] occurs at $(2\beta, \beta_A) \simeq (1.57 \pm 0.05, 0.78 \pm 0.05)$.

The $O(\delta^3)$ calculation (free energy) simply confirms the order-by-order convergence of the LDE to the MC results. The phase transition point on the SO(3) axis now coincides with the MC point at $\beta_A \simeq 2.5$. The Z_2 transition is localized around $2\beta \simeq 0.44$, while we locate the triple-point at $(2\beta, \beta_A) \simeq (0.535, 2.35)$ compared to the MC point $(2\beta, \beta_A) \simeq (0.55 \pm 0.03, 2.34 \pm 0.03)$. The end-point at this order is estimated at $(2\beta, \beta_A) \simeq (1.56, 0.82)$. All our phase diagrams are shown in figs. (1–3). MC points have been extracted from ref. [9].

To conclude this section, we make a few remarks about the end-point, which is an important feature of the phase structure of the mixed SU(2)-SO(3) lattice gauge system. According to the argument presented in ref. [24], the end-point of first-order phase transitions in mixed fundamental-adjoint SU(N) lattice gauge theories should occur above the line

$$\beta_A + \frac{N^2 - 1}{2N^2}\beta \cos(2\pi/N) = 0, \tag{19}$$

below which the nontrivial local minima of the one-plaquette action become unstable.

In our optimization scheme, the end-point $(2\beta^c, \beta_A^c)$ occurs where the system just enters entirely into the weak-coupling region, with PMS points now appearing for all $(2\beta, \beta_A)$ as we move away from the end-point towards the fundamental SU(2) axis. In particular, since we are in the weak-coupling region, the free energy remains negative and no longer changes sign as we vary β_A down to $\beta_A = 0$ for any $\beta > \beta^c$. Hence there are no more first-order phase transitions between the strong-coupling and the weak-coupling regions. Notice that our end-point coordinates are in excellent agreement with the criterion of eq. (19).

[†] Ref. [9] quotes $(1.48 \pm 0.05, 0.9 \pm 0.03)$, but both the diagram in that paper and ref. [10] give $(1.57 \pm 0.05, 0.78 \pm 0.05)$ for the end-point.

4. Conclusions

In this paper we have sought to extend the range of applications of the linear delta expansion within the context of lattice gauge theory. Hitherto the method has been applied only to the plaquette energy, for U(1) [5] and pure SU(2) systems [6–8]. In principle the choice of trial action should ultimately be immaterial, but of course in practice it is important to choose a trial action which gives rapid convergence.

From this and previous studies it seems that the trial action S_0 based on single links [25] is suitable for a wide variety of situations (although in the strong-coupling régime of lattice SU(2), an action based on a maximal tree of plaquettes [7] gives rather better results for E_P). The method developed in the appendix for evaluating higher-order correlations makes it feasible for such calculations to be carried out even when the number of plaquettes involved is quite large.

As in previous applications of the method, the role of the PMS criterion is crucial. It is this aspect of the method which makes it truly non-perturbative, although the methodology prior to optimization is perturbative in nature. As mentioned in the introduction, the PMS is also crucial for the convergence of the expansion. This is certainly the case in practice, and it has now been proved analytically [3,4] in zero and one dimensions.

One can therefore be optimistic about the prospects for applying the method to further aspects of lattice gauge theory, such as finite temperature, string tension, mass gap etc. We shall be investigating some of these aspects in future papers.

Appendix

In ref. [25], a method was given for evaluating the expectation values of plaquette diagrams w.r.t. the single-link trial action, S_0 based on the group integration technique of Creutz [26]. This method becomes increasingly tedious, making progress exceedingly difficult beyond diagrams involving four plaquettes, for example beyond $O(\delta^3)$ in calculating the plaquette energy of the SU(2) system. In this appendix, we present a simpler technique and a set of identities for calculating these expectation values to any desired order. We also illustrate how to handle the Z_2 degrees of freedom in the calculations.

SU(2)

We shall include only the important steps. We note at the outset that our single-link trial partition function $Z_0 = \int \prod_\ell dU_\ell \exp(\sum_\ell \text{tr}\,(J_\ell U_\ell))$, where we have taken $J_\ell = J$ as constant in our calculations, is basically a generating function for group integrals, and we can therefore obtain values of group integrals by successive differentiations of Z_0 w.r.t. J. The starting point in the calculation of plaquette diagram expectation values is that for a single link element in the order n calculation, we have the simple formula

$$< (\text{tr}\, U)^n >_0 = \int \prod_\ell dU_\ell e^{S_0} (\text{tr}\, U)^n$$
$$= \frac{1}{f(J)} \frac{d^n f(J)}{dJ^n}. \qquad (A1)$$

For the SU(2) group,

$$f(J) = \frac{I_1(2J)}{J}.$$

Denoting $\omega_n =< (\text{tr}\, U)^n >_0$, and performing the calculation in eq. (A1), we find the following general form:

$$\omega_n = \alpha_1 V_{n+1} + \alpha_2 V_{n-1} + ... + \alpha_k V_L. \qquad (A2)$$

with $V_r = I_r(2J)/I_1(2J)$. The order of the modified Bessel functions, r, decreases in steps of 2 down to $L = 2$ (1) for n odd (even). The coefficients α_i obey the simple relations:

$$\alpha_1 = (n+1); \qquad \alpha_2 = (n-1)^2; \qquad \text{and} \sum_{i=1}^{k} \alpha_i = 2^n. \qquad (A3)$$

A few illustrative examples may be useful;

$$\omega_1 = 2V_2$$
$$\omega_2 = 3V_3 + 1$$
$$\omega_3 = 4V_4 + 4V_2$$
$$\omega_4 = 5V_5 + 9V_3 + 2$$

etc. Notice that the coefficients in each case obey eq. (A3) above.

With ℓ links under the trace, we find the general property,

$$< (\text{tr}\,(U_1 U_2 .....U_\ell))^n >_0 = \alpha_1 V_{n+1}^\ell + ... + \alpha_k V_L^\ell. \qquad (A4)$$

For a closed loop of links, ℓ is the perimeter of the loop. This property is crucial in evaluating plaquette diagram expectation values, as we explain below. Consider first the case $\ell = 2$. Eq. (A4) gives immediately

$$\begin{aligned} < \text{tr}\,(U_1 U_2) >_0 &= 2V_2^2 \\ < (\text{tr}\,(U_1 U_2))^2 >_0 &= 3V_3^2 + 1 \\ < (\text{tr}\,(U_1 U_2))^3 >_0 &= 4V_4^2 + 4V_2^2 \\ < (\text{tr}\,(U_1 U_2))^4 >_0 &= 5V_5^2 + 9V_3^2 + 2 \end{aligned} \qquad (A5)$$

etc. Identifying $V_2 = \omega_1, V_3 = \Omega, V_4 = \Lambda$ and $V_5 = (\omega_4 - 3\omega_2 + 1)/5$ in the notation of ref. [25], eqs. (A5) are exactly the results obtained with the previous method, which also obscured the simple relation involving V_5 above. For n plaquettes sharing all four links ($\ell = 4$), we have

$$\begin{aligned} < \text{tr}\, U_P >_0 &= 2V_2^4 \\ < (\text{tr}\, U_P)^2 >_0 &= 3V_3^4 + 1 \\ < (\text{tr}\, U_P)^3 >_0 &= 4V_4^4 + 4V_2^4 \\ < (\text{tr}\, U_P)^4 >_0 &= 5V_5^4 + 9V_3^4 + 2 \end{aligned} \qquad (A6)$$

etc., which are the expressions for diagrams D_{11}, D_{21}, D_{31} and D_{41} respectively in ref. [25]. It is thus very easy to calculate the expectation values of plaquettes sharing all four links, i.e., plaquettes occupying the same location on the lattice. Diagrams in which plaquettes share fewer than four links in all possible ways can be evaluated by noting that the general property in eq. (A4) is obtained by integrating over each link successively. By keeping mathematical complications to a minimum, we adopt a simple way to recover the integration over a given link, e.g.,

$$< \text{tr}\, U >_0 = 2V_2 \Rightarrow V_2 = \frac{1}{2} < \text{tr}\, U >_0$$
$$< (\text{tr}\, U)^2 >_0 = 3V_3 + 1 \Rightarrow V_3 = \frac{1}{3} < (\text{tr}\, U)^2 - 1 >_0$$

etc., so that in eq. (A5) we can write

$$< \text{tr}\,(U_1 U_2) >_0 = \frac{1}{2} < \text{tr}\, U_1 >_0 < \text{tr}\, U_2 >_0$$

$$< (\mathrm{tr}\,(U_1U_2))^2 >_0 = \frac{1}{3} < [(\mathrm{tr}\,U_1)^2(\mathrm{tr}\,U_2)^2 - (\mathrm{tr}\,U_1)^2 - (\mathrm{tr}\,U_2)^2 + 4] >_0$$

etc., which are the identities calculated in ref. [25]. By carrying out such elementary steps and integrating completely over only one link in each case, we derive the following identities:

(i)

$$< \mathrm{tr}\,(U_1U_2) >_0 = < V_2 \mathrm{tr}\,U_2 >_0$$

(ii)

$$< (\mathrm{tr}\,(U_1U_2))^2 >_0 = < V_3[(\mathrm{tr}\,U_2)^2 - 1] + 1 >_0$$

(iii)

$$< (\mathrm{tr}\,(U_1U_2))^3 >_0 = < V_4[(\mathrm{tr}\,U_2)^3 - 2\mathrm{tr}\,U_2] + 2V_2\mathrm{tr}\,U_2 >_0$$

(iv)

$$< (\mathrm{tr}\,(U_1U_2))^4 >_0 = < V_5[(\mathrm{tr}\,U_2)^4 - 3(\mathrm{tr}\,U_2)^2 + 1] + 3V_3[(\mathrm{tr}\,U_2)^2 - 1] + 2 >_0 \quad (A7)$$

(v)

$$\begin{aligned} < (\mathrm{tr}\,(U_1U_2))^5 >_0 = & < V_6[(\mathrm{tr}\,U_2)^5 - 4(\mathrm{tr}\,U_2)^3 + 3\mathrm{tr}\,U_2] \\ & + 4V_4[(\mathrm{tr}\,U_2)^3 - 2\mathrm{tr}\,U_2] + 5V_2\mathrm{tr}\,U_2 >_0 \end{aligned}$$

(vi)

$$\begin{aligned} < (\mathrm{tr}\,(U_1U_2))^6 >_0 = & < V_7[(\mathrm{tr}\,U_2)^6 - 5(\mathrm{tr}\,U_2)^4 + 6(\mathrm{tr}\,U_2)^2 - 1] \\ & + 5V_5[(\mathrm{tr}\,U_2)^4 - 3(\mathrm{tr}\,U_2)^2 + 1] + 9V_3[(\mathrm{tr}\,U_2)^2 - 1] + 5 >_0 \end{aligned}$$

Using the recurrence relation for group characters,

$$\chi_{q+\frac{1}{2}}(U) = \chi_q\chi_{\frac{1}{2}}(U) - \chi_{q-\frac{1}{2}}(U)$$

we can write these identities in terms of the characters $\chi_{q+\frac{1}{2}}(U)$ of the various representations $q + \frac{1}{2}$ of the SU(2) gauge group. For example, the identity (vi) can be written in terms of characters in the form:

$$< (\mathrm{tr}\,(U_1U_2))^6 >_0 = < V_7\chi_3(U_2) + 5V_5\chi_2(U_2) + 9V_3\chi_1(U_2) + 5 >_0$$

In each case the highest representation is $n/2$. As a by-product of our elementary step in recovering link integrations, we obtain the following general result:

$$< \chi_j(U) >_0 = (2j+1)V_{2j+1}$$

A general trend thus emerges which we can use to generate as many of such identities as we desire. Together with the identities we have given in ref. [8], the above are enough to evaluate diagrams of up to $n = 7$ plaquettes connected in all possible ways. The first four identities above are exactly the same as the results in ref. [25] with the link element U_1 integrated out completely. Through the process of successive integrations using the identities, we note that each link element integrated out contributes an appropriate factor V_r.

We now give the expressions for the remaining diagrams used in eqs. (14–16):

$$\begin{aligned} C_1 &= < \mathrm{tr}\,U_P >_0 = 2V_2^4 \\ D_{22} &= < \mathrm{tr}\,(U_1U_2U_3^+U_4^+)\,\mathrm{tr}\,(U_5U_6U_7^+U_2^+) >_0 = V_2^6\omega_2 \\ D_{32} &= < (\mathrm{tr}\,(U_1U_2U_3^+U_4^+))^2\,\mathrm{tr}\,(U_5U_6U_7^+U_2^+) >_0 \\ &= V_2^3[V_3^3(\omega_3 - 2V_2) + 2V_2] \qquad (A8) \\ D_{43} &= < (\mathrm{tr}\,(U_1U_2U_3^+U_4^+))^2(\mathrm{tr}\,(U_5U_6U_7^+U_2^+))^2 >_0 \\ &= V_3^6(\omega_4 - 2\omega_2 + 1) + 6V_3^4 + 1 \end{aligned}$$

As observed earlier, in the limit $J = \infty$, all $V_r = 1$ and eqs. (15), (16), (A6) and (A8) give the Z_2 result, eq. (17).

Z_2 Elements

To handle Z_2 degrees of freedom, we use the formula

$$< (\sigma_\ell)^n >_0 = \frac{1}{g(m)}\frac{d^n g(m)}{dm^n}$$

with the general result

$$< (\sigma_\ell)^n >_0 = t \text{ or } 1$$

for n odd or even respectively. For the single-link Z_2 trial action adopted here, $g(m) = \cosh m$ and $t = d(\log g)/dm = \tanh m$.

We use the following examples to illustrate the calculation of connected expectations in our mixed model:

$$\begin{aligned} < \mathrm{tr}\,(U_P\sigma_P) >_0 &= < \mathrm{tr}\,U_P >_0 < \sigma_P >_0 = C_1t^4 \\ < (\mathrm{tr}\,(U_P\sigma_P))^2 >_0 &= < (\mathrm{tr}\,U_P)^2 >_0 < (\sigma_P)^2 >_0 = D_{21} \qquad (A9) \\ < (\mathrm{tr}\,(U_P\sigma_P))^2 >_C &= < (\mathrm{tr}\,(U_P\sigma_P))^2 >_0 - < \mathrm{tr}\,(U_P\sigma_P) >_0^2 = D_{21} - C_1^2t^8 \end{aligned}$$

Finally, based on the general properties eqs. (A2)–(A4), the following observations are important.

(a) In the limit $J = \infty$,

$$< (\mathrm{tr}\,U_P)^n >_0 = 2^n. \qquad (A10)$$

In fact, for n plaquettes connected in all possible ways, we have

$$< \prod_{i=1}^{n} \mathrm{tr}\, U_{P_i} >_0 = 2^n$$

at $J = \infty$. Connected expectation values are zero in this limit, i.e.,

$$< \prod_{i=1}^{n} \mathrm{tr}\, U_{P_i} >_C = 0$$

at $J = \infty$ except for the case $n = 1$, which gives $< \mathrm{tr}\ U_P >_C = < \mathrm{tr}\ U_P >_0 = 2$ in this limit. As a consequence, the plaquette energy of the SU(2) system becomes $E_P = < \frac{1}{2} \mathrm{tr}\ U_P > = 1$ at $J = \infty$.

(b) In the limit $J = 0$, all $V_r = 0$ and

$$< (\mathrm{tr}\ U_P)^n >_0 = \alpha_k. \qquad (A11)$$

We know that at $J = 0$, $< (\mathrm{tr}\ U_P)^n >_0 = \int \prod_\ell dU_\ell (\mathrm{tr}\ U_P)^n$ leads directly to the strong-coupling limit of the system. In fact, the result, α_k, obtained from eq. (A11) is exactly the same as the SU(2) character expansion result [12],

$$\int \prod_\ell dU_\ell (\frac{1}{2} \mathrm{tr}\ U_P)^n = C \left[\frac{(n-1)!!}{n!!} - \frac{(n+1)!!}{(n+2)!!} \right] \qquad (A12)$$

where the constant $C = 4/\pi$ or 2 for n odd or even respectively. Note that the term in square brackets can be simplified to $[(n-1)!!/(n+2)!!]$. This identity (A12) suggests a direct link between the strong-coupling limit we obtain with the single-link trial action and the strong-coupling character expansion. The connected expectation values of plaquettes sharing all four links is equal to a constant for n even and zero for n odd at $J = 0$. Similarly the connected expectation values of all plaquettes sharing fewer than four links are zero at $J = 0$. That is,

$$< (\mathrm{tr}\ U_P)^n >_C = \text{constant}$$

and

$$< \prod_{i=1}^{n} (\mathrm{tr}\ U_{P_i}) >_C = 0 \qquad \text{at } J = 0. \qquad (A13)$$

References

1. A. Duncan and M. Moshe: *Phys. Lett.* **215B** (1988) 352. For a recent review see H. F. Jones in *Proceedings of LP-HEP 91*, p.111 (World Scientific, 1992).
2. P. M. Stevenson: *Phys. Rev.* **D23** (1981) 2916.
3. I. R. C. Buckley, A. Duncan and H. F. Jones: Imperial College preprint TP/91-92/24, to be published in Physical Review D.
4. A. Duncan and H. F. Jones: Imperial College preprint TP/91-92/29, to be published in Physical Review D.
5. A. Duncan and H. F. Jones: *Nucl. Phys.* **B320** (1989) 189.
6. I. R. C. Buckley and H. F. Jones: *Phys. Rev.* **D45** (1992) 654.
7. I. R. C. Buckley and H. F. Jones: *Phys. Rev.* **D45** (1992) 2073.
8. J. O. Akeyo and H. F. Jones: Imperial College preprint TP/91-92/27, to be published in Physical Review D.
9. M. Creutz and G. Bhanot: *Phys. Rev.* **D24** (1981) 3212.
10. M. Creutz: *Quarks, Gluons and Lattices*, CUP 1983.
11. L. Caneschi, I. G. Halliday and A. Schwimmer: *Nucl. Phys.* **B200 [FS4]** (1982) 409; I. G. Halliday and A. Schwimmer: *Phys. Lett.* **102B** (1981) 337.
12. R. C. Brower, D. A. Kessler and H. Levine: *Nucl. Phys.* **B205 [FS5]** (1982) 77.
13. M. Baig and A. Cuervo: *Nucl. Phys.* **B280 [FS18]** (1987) 97.
14. S. J. Anthony: *Phys. Lett.* **110B** (1982) 271.
15. J. B. Kogut, J. Polonyi and H. W. Wyld: *Phys. Rev.* **D31** (1985) 3304.
16. J. M. Drouffe: *Phys. Lett.* **105B** (1981) 46; *Nucl. Phys.* **B205 [FS4]** (1982) 27.
17. D. J. Pritchard: *Phys. Lett.* **106B** (1981) 193.
18. X. Zheng, C. I. Tan and T. Chen: *Phys. Rev.* **D26** (1982) 2843.
19. J. M. Alberty, H. Flyvberg and B. Lautrup: *Nucl. Phys.* **B220 [FS8]** (1983) 61.

20. H. Ceccato, E. Dagotto and A. Moreo: *Phys. Rev.* **D31** (1985) 1465.

21. E. Dagotto and A. Moreo: *Phys. Rev.* **D30** (1984) 1271.

22. R. Dashen, U. M. Heller and H. Neuberger: *Nucl. Phys.* **B215 [FS7]** (1983) 360.

23. K. M. Bitar, S. Gottlieb and C. K. Zachos: *Phys. Rev.* **D26** (1982) 2853.

24. C. P. Bachas and R. F. Dashen: *Nucl. Phys.* **B210 [FS6]** (1982) 583.

25. X. Zheng, Z. G. Tan and J. Wang: *Nucl. Phys.* **B287** (1987) 171.

26. M. Creutz: *J. Math. Phys.* **19** (1978) 2043.

Figure Captions

Fig. 1 Phase Structure from F to $O(\delta)$

Fig. 2(a) Phase Structure from F to $O(\delta^2)$

Fig. 2(b) Phase Structure from E_P to $O(\delta)$

Fig. 3 Phase Structure from F to $O(\delta^3)$

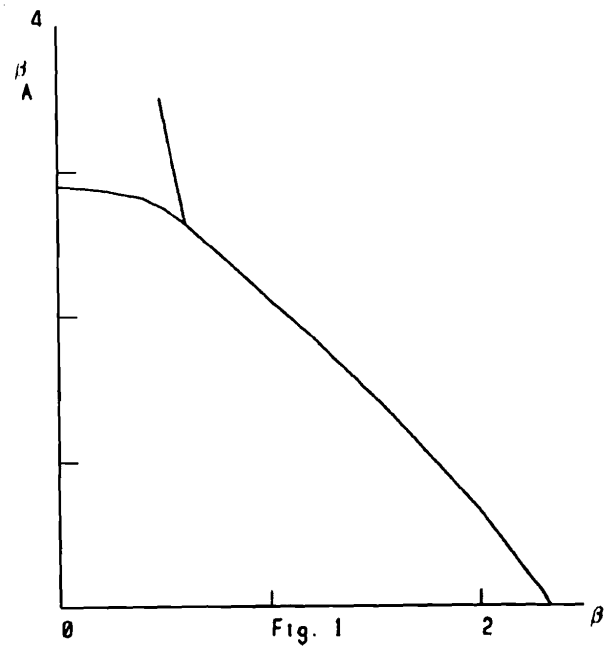

Fig. 1

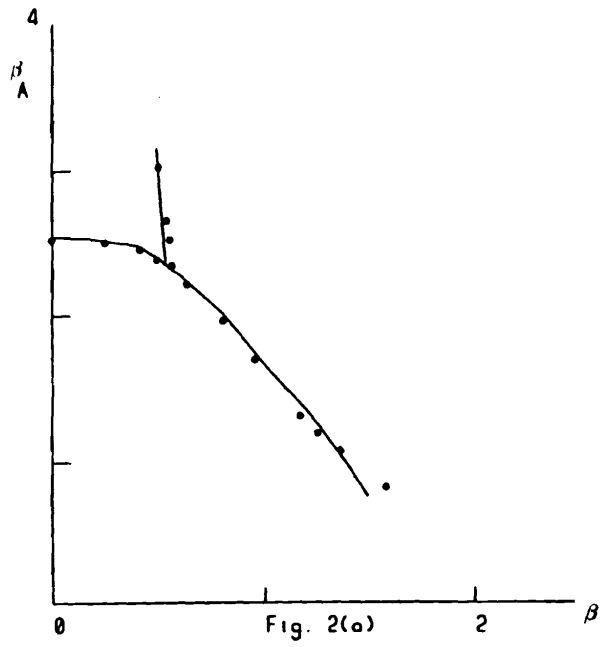

Fig. 2(a)

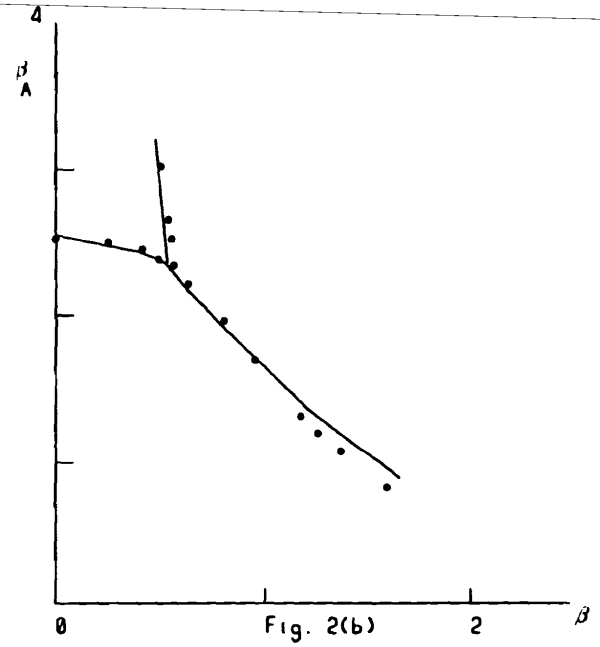

Fig. 2(b)

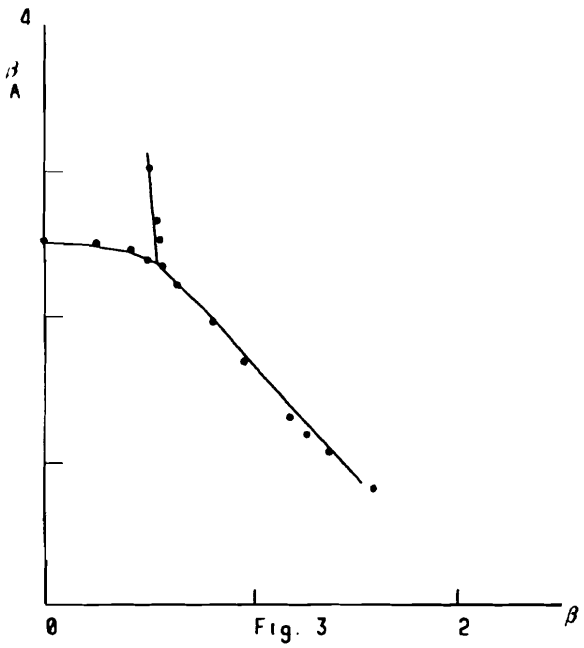

Fig. 3